Front. Environ. Sci. Eng. 2018, 12(4): 9
https://doi.org/10.1007/s11783-018-1066-3

RESEARCH ARTICLE

Immobilization of NZVI in polydopamine surface-modified biochar for adsorption and degradation of tetracycline in aqueous solution

Xiangyu Wang[1], Weitao Lian[1], Xin Sun[1], Jun Ma[2], Ping Ning (✉)[1]

1 Faculty of Environmental Science and Engineering, Kunming University of Science and Technology, Kunming 650500, China
2 School of Municipal and Environmental Engineering, State Key Laboratory of Urban Water Resources and Environment, Harbin Institute of Technology, Harbin 150090, China*

HIGHLIGHTS

- Novel method for polydopamine (PDA) modified biochar (BC) with immobilized NZVI.
- PDA/NZVI@BC exhibits significantly enhanced activity for tetracycline (TC) removal.
- TC removal efficiency was increased by 55.9% compared with that of pristine NZVI.
- The mechanism of tetracycline removal by PDA/NZVI@BC was proposed.

GRAPHIC ABSTRACT

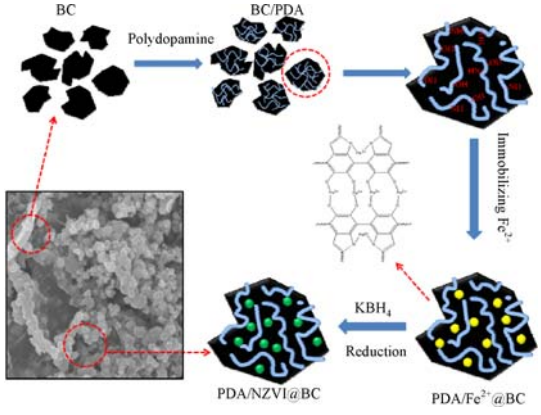

ARTICLE INFO

Article history:
Received 10 February 2018
Revised 11 May 2018
Accepted 20 June 2018
Available online 4 August 2018

Keywords:
Biochar
Polydopamine
NZVI
Modification
Tetracycline

ABSTRACT

Polydopamine/NZVI@biochar composite (PDA/NZVI@BC) with high removal efficiency of tetracycline (TC) in aqueous solutions was successfully synthesized. The resultant composite demonstrated high reactivity, excellent stability and reusability over the reaction course. Such excellent performance can be attributed to the presence of the huge surface area on biochar (BC), which could enhance NZVI dispersion and prolong its longevity. The carbonyl group contained on the surface of biochar could combine with the amino group on polydopamine(PDA). The hydroxyl groups in PDA is able to enhance the dispersion and loading of NZVI on BC. Being modified by PDA, the hydrophilicity of biochar was improved. Among BC, pristine NZVI and PDA/NZVI@BC, PDA/NZVI@BC exhibited the highest activity for removal of TC. Compared with NZVI, the removal efficiency of TC could be increased by 55.9% by using PDA/NZVI@BC under the same conditions. The optimal modification time of PDA was 8h, and the ratio of NZVI to BC was 1:2. In addition, the possible degradation mechanism of TC was proposed, which was based on the analysis of degraded products by LC-MS. Different important factors impacting on TC removal (including mass ratio of NZVI to BC/PDA, initial concentration, pH value and the initial temperature of the solution) were investigated as well. Overall, this study provides a promising alternative material and environmental pollution management option for antibiotic wastewater treatment.

1 Introduction

In the aquatic environment, antibiotics are extensively and significantly concerned because of their widespread occurrence and potential risks to aquatic organisms and human health (Daghrir and Drogui, 2013; Rodriguez-

✉ Corresponding author
E-mail: ningping58_2015@sina.com

*Special Issue—Bio-based Technologies for Resource Recovery (Responsible Editors: Aijie Wang & David Stuckey)

Mozaz et al., 2015). Tetracycline (TC), as one of the broad-spectrum antibiotics, is widely used in medical treatment and livestock breeding and aquaculture (Chen and Wang, 2009; Jeong et al., 2010; Yang et al., 2015). In recent years, TC has been frequently detected in wastewater, surface water, soil and ground water with direct or indirect way (Sarmah et al., 2006). TC can pose a potential risk for the drinking water safety and human health. The general techniques were used for removal of TC in wastewater, such as adsorption, photodegradation, reduction, and biological methods. Nano zero-valent iron (NZVI) has received great concerns in groundwater treatment and soil remediation due to its large specific surface area, high reactivity, and low cost for the removal of a various of pollutants (Li et al., 2015c), such as heavy metals (Arshadi et al., 2014; Li et al., 2015a), nitrobenzene (Yin et al., 2012a;2012b), chlorinated organic compounds (COCs) (He and Zhao, 2008; Wang et al., 2008; Su et al., 2011; Cao et al., 2015; Li et al., 2015b; Shen et al., 2017) and antibiotics (Ghauch et al., 2009). However, there are some problems that inhibit the application of NZVI technology, such as the agglomeration of NZVI particles (Guan et al., 2015; Dong et al., 2016) and the oxidation of NZVI particles (Feng et al., 2008). To control the particles agglomeration, various solid supports have been applied to stabilize nanoparticles, such as bentonite (Shi et al., 2011), metal oxides (Hsieh et al., 2010), membranes (Wang et al., 2008), activated carbon (Zhu et al., 2009), azolla (Arshadi et al., 2017), carboxymethyl cellulose (Cai et al., 2018), and biochar (BC) (Su et al., 2016b). Compared with other materials, BC has some distinct advantages, such as higher specific surface area, more stable structures capacity, greater adsorb ability and environment friendliness. BC can be easily prepared by using carbon-rich biomass as raw materials via pyrolysis under low oxygen conditions (Chen et al., 2008). Besides, BC can also prevent the oxidization of NZVI and overcome the agglomeration of NZVI. Meanwhile, BC can provide large surface area for immobilization and dispersion of nanoparticles. In previous studies, Lyu et al. (2018) used biochar supported nanoscale iron sulfide composite to immobilize hexavalent chromium in contaminated soils.

NZVI was successfully loaded onto BC to form hybrid structures, and it can effectively enhance the removal of chromium (Su et al., 2016a; 2016b). Dong et al. further modified biochar by hydrochloric acid to stable NZVI for Cr(VI) removal from aqueous solution. However, the removal efficiency of Cr(VI) was only about 45% (Dong et al., 2017). Recently, 3,4-dihydroxyphenethylamine(dopamine) had attracted much attention as a powerful building block to form strong adhesive interaction with various substrates in wet environment (Sever et al., 2004). 3,4-dihydroxyphenethylamine(dopamine) or its derivatives (such as 3,4-dihydroxyphenylalanine) is becoming a promising surface modification material (Lee et al., 2007). Due to the abundant catecholgroups and ethylamino groups, dopamine can self-polymerize on the substrate surface to form a hydrophilic polymer(i.e., Polydopamine (PDA)) layer. During the reaction, a tightly adherent PDA layeris generated on a substrate by creating nano-sized spherical PDA product in the solution (Jiang et al., 2013). The modified surfaces played an important role as useful platforms for secondary reactions and surface functionalization with mild conditions (Xi et al., 2009). The property of PDA for self-polymerizing was used for the modification of material surfaces in wastewater, such as TiO_2 nanoparticles (Shao et al., 2012), graphene (Loget et al., 2015) and clay (Yang et al., 2011), to enhance interfacial interactions between nano materials and polymer matrices. Meanwhile, because PDA can significantly increase interfacial interactions between nano materials and polymer matrices, the interfacial PDA layers effectively promote the dispersion of these nanoparticles (Yu et al., 2013). Furthermore, this material can be applied for the modification of carbon nanotubes(Zabihi and Araghi, 2016a; 2016b).

In this study, the PDA/NZVI@BC composites were innovatively synthesized. The objective of this research work is to enhance the dispersion and activity of NZVI by using the as-prepared novel PDA/NZVI@BC composite. Comparatively, biochar was synthesized by the method of pyrolysis of rice shell in tube furnace with nitrogen environment. Then a hydrophilic polymerlayer was formed through self-polymerization of dopamine on the BC surface, and NZVI was coated on the surface of PDA modified BC by liquid phase reduction method. During this process, BC acted as a mesoporous support substrate, and PDA was an effective modifier to significantly increase the interfacial interactions between NZVI and BC. Meanwhile, the method of liquid phase reduction excellently controlled the size of NZVI.

2 Materials and methods

2.1 Materials

All reagents were of analytical reagent grade or above unless otherwise stated and used as received without further purification. Ferrous sulfate heptahydrate ($FeSO_4 \cdot 7H_2O$) and HNO_3 were supplied by Sinopharm Chemical Reagent Co. Ltd (Shanghai, China). Potassium borohydride (KBH_4) were obtained from Kelong Chemical Reagent Co. Ltd (Chengdu, China). PDA was purchased from Sigma-Aldrich and used as received. Tris(hydroxymethyl) aminomethane (Tris) is obtained from Sinopharm Chemical Reagent Co. Ltd. Tetracycline (TC) was purchased from Aladdin Chemistry (Shanghai, China).The chemicals are used without further purification. Rice-husk was gathered from a farm of Hefei, south-east of China. All the biomass materials were crushed by a high speed rotary cutting mill, screened to limit the particle size in range of

40−60 mesh and dried at 100°C for 7 h to remove the moisture. Ultrapure water was used in all experiments for preparation of various reagent solutions.

2.2 Biomass pyrolysis and pretreatment of the obtained biochar

The pyrolysis processes were performed at temperatures of 500°C using tube furnace. The crude biochars were washed by diluted HNO_3 (0.1 mol/L) at room temperature to remove the acid-leachable impurity, followed by H_2O elution until the pH of the washing liquid was about 7.0. The wet biochars were then heated at 100°C for 4 h and stored in desiccators for further use. (Tan et al., 2017)

2.3 Modification of BC

PDA solution was prepared by dissolving dopamine in Tris-HCl (1.0 g/L). The concentration of PDA solution was 2.0 g/L. BC sample (0.5 g) was immersed into the PDA solution and vibrated at 30°C for a designed coating time. Then the PDA modified BC (BC/PDA) was taken out and washed with deionized water for 24 h. After dried to a constant weight at 40°C in vacuum oven, the resultant modified BC was used for characterization.

2.4 Synthesis of PDA/NZVI@BC

The BC/PDA was added into 250 mL 0.054 M $FeSO_4$ solution with vigorous magnetic stirring. NZVI was prepared by adding 250 mL 0.138 M KBH_4 solution drop wise into $FeSO_4$ solution with vigorous magnetic stirring. And the solution was stirred for additional 30 min after KBH_4 was added into $FeSO_4$ solution completely. NZVI could be synthesized according to the following equation:

$$Fe^{2+} + 2BH_4^- + 6H_2O \rightarrow Fe^0 \downarrow + 2B(OH)_3 + 7H_2 \uparrow \quad (1)$$

The obtained PDA/NZVI@BC particles were rinsed 3 times with Milli-Q water and absolute ethanol, and dried in a vacuum drying oven under room temperature. Then, the prepared PDA/NZVI@BC was restored in vials for further characterization and degradation experiments. Liquid phase reduction method was employed for synthesis of PDA/NZVI@BC, and the typical preparation diagram of PDA/NZVI@BC is depicted in Fig. S1 (see it in Supplementary material).

2.5 Characterization of PDA/NZVI@BC

Scanning electron microscopy (SEM, Carl Zeiss Jena, Germany) images of BC, BC/PDA, PDA/NZVI@BC. Surface functional groups were characterized by a Fourier transform infrared spectroscope (FTIR, VERTEX 80v, Bruker, Germany), where samples were mixed with the KBr (1:30) and pressed into a sheer slice. The surface elements' valence and composition of the fresh and exhausted NZVI/BC was acquired by X-ray photoelectron spectrometer (XPS, ESCALAB 250Xi, Thermo Fisher, USA) with a source of Al K Alpha. The spectra calibrating binding energy was performed using C1s peak at 284.8 eV. X-ray diffraction (XRD, D8ADVANCE, Bruker, Germany) using Cu-Kα radiation at 40 kV/30 mA was used to analyze the crystal structure of particles.

2.6 Batch experiments

Batch experiments were performed in 60 mL sealed vials, each of which contained 50 mL of TC solution. And all experiments were conducted in duplicate under aerobic conditions by shaking back and forth at 30 rpm. The pH of reaction samples was adjusted by solutions of 0.1 M HCl and 0.05 M NaOH, and determined using a PHS-2F precision pH meter (Shanghai Precision Scientific Instruments Co., Ltd., China). TC reduction was initiated by 1.0 g/L PDA/NZVI@BC composite into a glass vial. At regular time intervals (up to 60 min), 2.5 mL of reaction samples were withdrawn for TC residue analysis. For the sake of comparison, an identical procedure was used to remove TC with freshly prepared NZVI only. In addition, parallel blank experiments were also conducted under the same conditions, with 1.0 g BC only, or without any materials in solution, to examine whether the adsorption of BC or the evaporation of TC would affect the removal of TC or not. Subsequently, a series of degradation experiments were also carried out under different initial concentrations of TC solution, pH values, and reaction temperatures to investigate the effects of environmental parameters on TC removal by PDA/NZVI@BC.

3 Results and discussion

3.1 Comparison of reactivities of BC, NZVI and PDA/NZVI@BC

Figure 1a shows the removal of TC in aqueous solution using BC, NZVI, BC/NZVI, and PDA/NZVI@BC under the same initial iron content (0.24 g/L), respectively. The removal efficiencies followed the order of PDA/NZVI@BC>BC/NZVI>NZVI>BC. The TC removal efficiency with BC was only 10.8% at 1 h, and the leading role of biochar was adsorption. Although biochar has a large specific surface area, the adsorption capacity is not strong enough due to the few surface functional groups. Due to the aggregation and oxidation of iron particles, the TC removal efficiency with pristine NZVI was found to increase quite slowly to 38.6% at 1 h. In addition, BC/NZVI can remove a certain amount of TC due to huge surface area of BC for dispersion and immobilization of

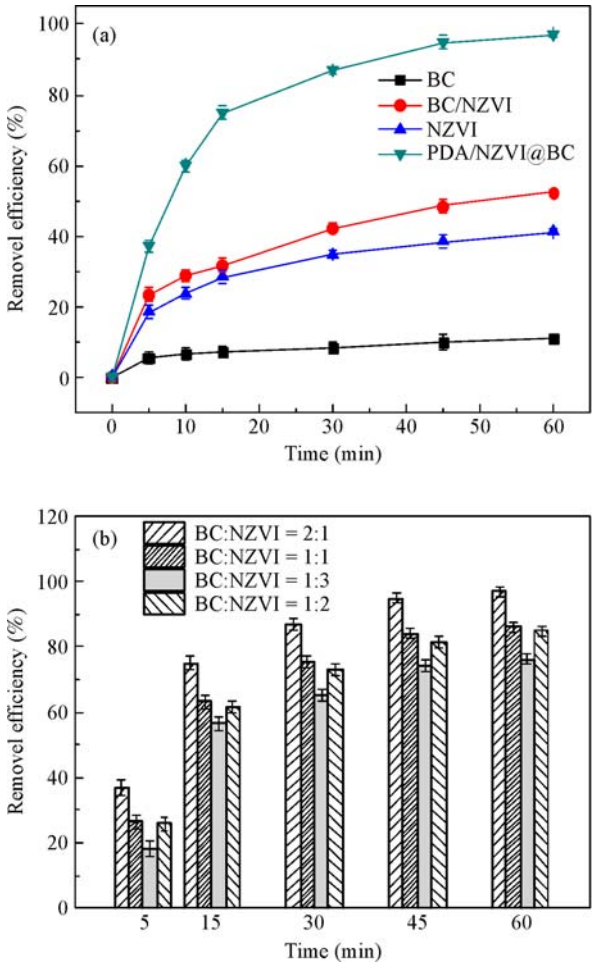

Fig. 1 (a) Comparison of removal efficiency of TC by BC, BC/NZVI, NZVI, and PDA/NZVI@BC (C_0 = 20 mg/L; BC dosage = 0.76 g/L, NZVI dosage = 0.24 g/L and PDA/NZVI@BC dosage = 1 g/L (NZVI: BC = 0.24: 0.76); t = 298 K); (b) Comparison of removal efficiency of TC by BC/NZVI with different mass ratio (C_0 = 20 mg/L; t = 298 K)

NZVI. However, only 41.2% TC was removed using BC/NZVI at 1 h due to the relative low dosage of NZVI loaded on the surface of BC. Most importantly, 98.28% of TC was removed from the solution within 1 h with PDA/NZVI@BC. The explanations for this phenomenon are: (1) the dispersion of NZVI particles could be improved by supporting it on the BC, which provides PDA/NZVI@BC with more accessible reactive sites for reduction of TC than the aggregated NZVI; (2) as an effective cross-linker, PDA enhanced the connection between BC and NZVI, because of the presence of amino and hydroxyl groups.

Figure 1b shows different mass ratio of BC/NZVI on TC removal. Under BC:NZVI = 1:3, the final removal efficiency was 76.8%. By further decreasing NZVI loading with the BC:NZVI ratio of 1:2, removal efficiency was slightly improved. At a ratio of 1:1, 86.5% TC was removed within 1 h with apparent improvement in the removal efficiency. This phenomenon is due to the fact that too much NZVI blocked the hole of BC at ratio of 1:3. The reason for this decrease might be that when the amounts of NZVI increased, the overdose of iron loading led to the aggregation of iron particles, thus resulting in the decrease removal efficiency. However, in the 2:1 case, the removal efficiency reached 98.7%. This may be due to the fact that the dispersion of NZVI is more likely to affect the degradation of TC than that the amount of NZVI. Therefore, the ratio of 2:1 for BC/NZVI was selected in the following characterization and degradation experiments.

3.2 Characterization of PDA/NZVI@BC composite

3.2.1 Surface morphologies

Figure 2 shows the representative SEM images of the as-synthesized BC, BC/PDA, and PDA/NZVI@BC. It can be observed from Fig. 2a that the BC surface is porous and has a regular shape. This provides a huge specific surface area. Figure 2b shows the structure of the enlarged BC hole. Figure 2c illustrates that PDA was well dispersed and attached on BC, indicating that the PDA as a modified material can effectively firmly and evenly secured on the BC surface that is beneficial to maintaining their high surface area and reactivity. The successful coating and immobilization of NZVI onto BC/PDA can be observed from Fig. 2d.

3.2.2 Surface functionality

The FTIR spectra (Fig. 3) were used to identify the functional groups presented in BC and PDA/NZVI@BC. The FTIR spectra for different materials were carried out in the range of 800–4000 cm^{-1}. Typically, the broad band around 3430 cm^{-1}corresponds to the O-H, the bands around 2923 cm^{-1} was assigned to aliphatic hydrocarbon C-H, the bands at about 1620 cm^{-1}, attributed to C = O vibration. The band at wavenumber near 1100 cm^{-1} assigned to the C-OH bending vibration, implying the existence of large numbers of hydroxyl groups (–OH) and carboxylate groups (–COOH) on the BC. In addition, comparing with the spectra of BC and PDA/NZVI@BC, after deposition of iron particles on carbon spheres, the intensity of the band at 3436 cm^{-1} and 1000–1500 cm^{-1} was weakened clearly, indicating the rupture of 500 partial OH bonds and implying the formation of C-O–Febonds. FTIR analyses further prove the existence of NZVI on the surfaces of BC/PDA.

3.2.3 Chemical composition

Figure 4 shows the XRD patterns of BC, NZVI, and PDA/

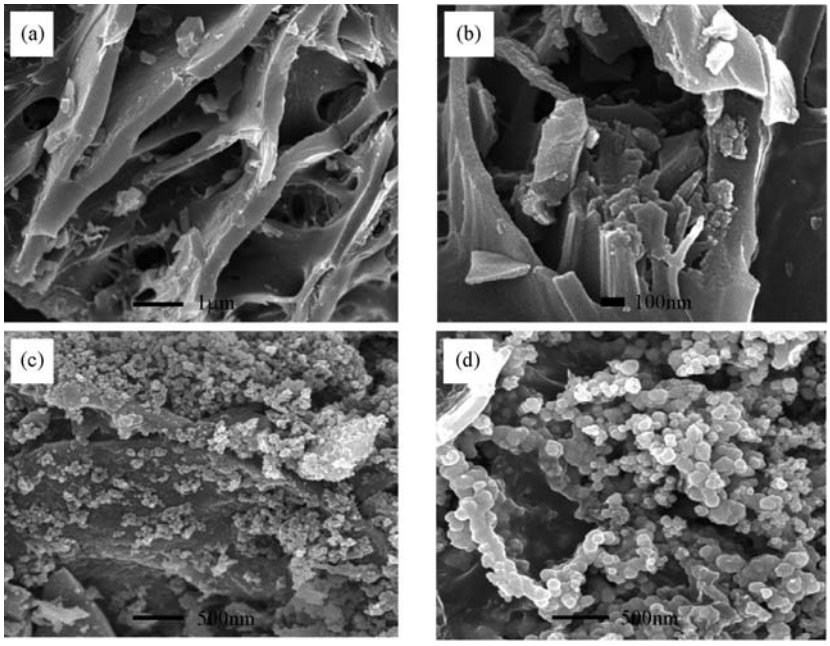

Fig. 2 SEM images of BC (a and b), BC/PDA (c), and PDA/NZVI@BC (d)

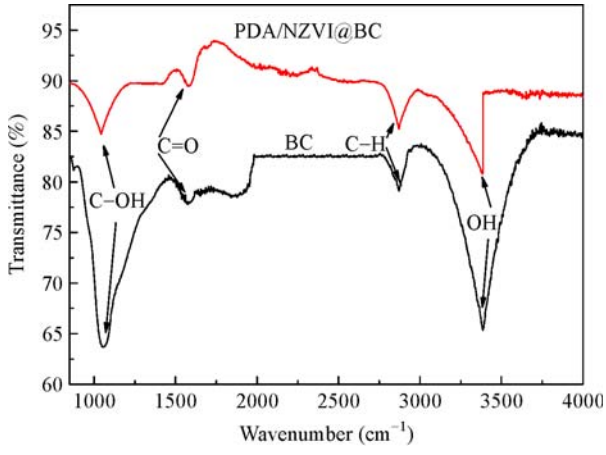

Fig. 3 FTIR spectra of BC and PDA/NZVI@BC

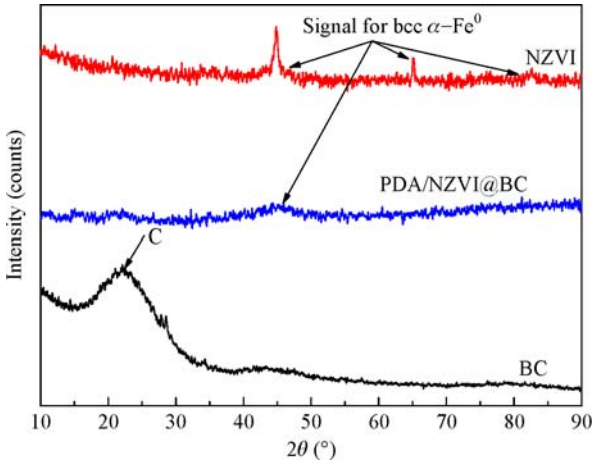

Fig. 4 XRD patterns of BC, BC/PDA, PDA/NZVI@BC, and NZVI

NZVI@BC composites. For BC, there was only a weak and broad peak at approximate $2\theta = 22°$, indicating that the carbon matrix was amorphous structure, which is consistent with other reported data. The signals of α-Fe^0 (characteristic peaks at 44.67°, 65.15°, and 82.53°) were detected obviously for NZVI. While for PDA/NZVI@BC, an apparent peak at $2\theta = 44.67°$ indicated the presence of NZVI. The XRD patterns reveal that the introduction of BC/PDA broadened the diffraction peaks and decreased their intensity, but did not lead to their crystal phase change, which was in agreement with previous findings. All of the above confirmed that NZVI was successfully loaded on the surface of BC/PDA. Besides, the presence of BC/PDA effectively decreased the aggregation of NZVI, resulting in high levels of stability and dispersity that enhanced their reactivity.

X-ray photoelectron spectroscopy (XPS) was employed for the investigation of the composition and chemical state of original BC, BC/PDA and PDA/NZVI@BC. Based on the full-range survey spectra (Fig. 5a), the major elements were consisted mainly of oxygen (O) and carbon (C). The appearance of Fe 2p on PDA/NZVI@BC composite substantially shows that the NZVI was well distributed in the compounds. Deconvolution of the C1s core-level spectrum of BC/PDA results in three peaks (Fig. 5b) at 288.6, 286.3 and 284.7 eV, which are assigned to C = O/COOH, C–N/C–OH and –CH–, respectively. Compare

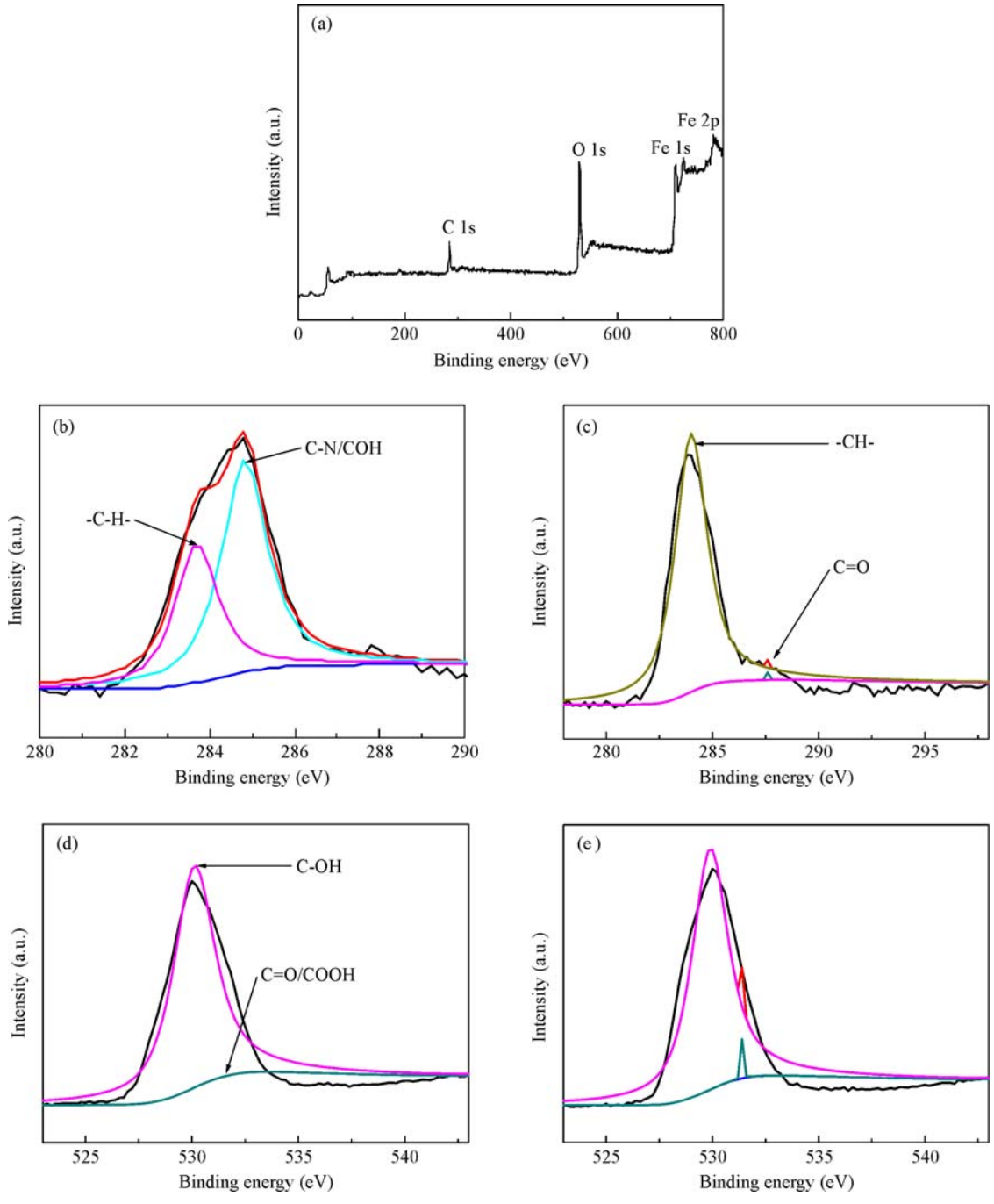

Fig. 5 Full-range XPS spectra of PDA/NZVI@BC (a); the XPS spectra of C 1s from the surfaces of BC/PDA (b); BC (c); the XPS spectra of O 1s from the surfaces of BC (d); BC/PDA (e)

with Fig. 5b, there is no the peak of C–N/C–OH in Fig. 5c. The presence of C-N/C-OH peaks is attributed to the amine groups on the BC/PDA surface formed by PDA self polymerization, and from the previous study of Ding et al., we can see that the carbonyl group contained on the surface of biochar can be combined with the amino group on dopamine, confirming the coating of PDA on BC (Ding et al., 2016). The O1s spectrum can be resolved into two typical peaks corresponding to C–OH (533.5 eV) and C = O/COOH (532.1 eV). In this respect, Figs. 5d and 5e are the same. This is due to these two peaks are characteristic peaks of BC. In summary, the successful coating of PDA layers and the uniform distribution of NZVI can be confirmed in XPS analysis result.

The BET surface areas (SA) of different types of biochars were compared (Table S1). The SA for the raw

Table 1 Fitted data for removal of TC by PDA/NZVI@BC using a two-parameter pseudo-first order decay kinetics model

C_0 (mg/L)	Dosage (g)	Initial (pH)	T (K)	Removal (%)	$C_{ultimate}$ (mg/L)	k (min^{-1})	R^2
20	0.2	5.58	298	97.19	0.265	0.1483	0.9989
25	0.2	5.58	298	96.13	5.066	0.0487	0.9962
30	0.2	5.58	298	84.32	15.430	0.0442	0.9948
35	0.2	5.58	298	81.20	32.216	0.0267	0.9861
20	0.2	2.53	298	80.23	13.256	0.0281	0.9960
20	0.2	4.16	298	92.60	12.230	0.0470	0.9763
20	0.2	7.33	298	99.02	0.082	0.0480	0.9988
20	0.2	8.45	298	82.80	31.828	0.0259	0.9895
20	0.2	5.58	288	30.30	132.956	0.0065	0.9847
20	0.2	5.58	308	96.40	4.494	0.0490	0.9937
20	0.1	5.58	298	89.96	10.634	0.0472	0.9909
20	0.3	5.58	298	97.70	0.174	0.0510	0.9978

biochars and those after various time modifications of PDA (8 h, 24 h) were 69.7 and 4.8 m^2/g, respectively. It appeared that the SA of BC/PDA(8 h) was much higher than that of the others. The phenomenon was due to the PDA polymerized on the surface of BC. The SA for BC/PDA (8 h)/NZVI was 78.5m^2/g, which is due to the NZVI loaded on the surface of PDA.

3.3 Effect of different reaction conditions

The effect of initial TC concentration on the removal process of TC was examined in the ranging from 10 to 50 mg/L. As shown in Fig. 6a, the degradation efficiency of TC was 96.15% at an initial TC concentration of 10 mg/L in 90 min, while at an initial concentration of 50 mg/L, only 67.14% TC was removed. Obviously, the removal efficiency of TC decreased with the increase of initial TC concentration. Similar results were also reported in other studies. The reasonable explanation is that the decrease amount of initial concentration can provide more availability of reactive sites for TC on PDA/NZVI@BC surface in the case of the fixed number of reactive sites, and the increased reaction rate subsequently resulted in the increase of k. Similar results concerning the effect of initial concentration of pollutant were also reported in previous.

The effect of solution pH on the removal process of TC is shown in Fig. 6b. The initial pH was adjusted to 8.45, 7.33, 5.58, 4.16, and 2.53, respectively. The removal efficiency was obviously increased as the pH decreased. At initial pH of 2.53, 4.16, 5.58, 7.73 and 8.45 of the TC in the solution was removed within 90 min. After 90 min, the removal efficiencies were found to be 99.16%, 99.03%, 96.79%, 88.56% and 85.95%, respectively. The reasons may be that: (1) at lower pH values, the iron oxidation could be accelerated, leading to generation of plenty of hydrogen (or hydrogen atoms), which promote the reduction of TC; (2) at pH higher than 7, the iron surface tends to form a passivation layer of iron hydroxide and build up on the surface of NZVI and BC, this hinders the transport of contaminants between NZVI and BC. This also further explained that the removal efficiency of PDA/NZVI@BC increased under the condition of acidic. Considering the removal efficiency of TC and practical application, the appropriate pH was selected for 5.58, TC removal was also found to be affected by solution temperature.

As shown in Fig. 6c, the removal efficiency of TC by PDA/NZVI@BC increased as the solution temperature increased at a certain temperature range. The removal efficiency of TC was 28.55% at 288 K, 90.17% at 298 K, and 93.57% at 308 K after 8 min of the degradation of TC. Obviously, it is evident that the removal efficiency of TC by PDA/NZVI@BC increased as the higher solution temperature. The explanation of this phenomenon is that the diffusion and mobility of TC molecules from the liquid phase transfer to the surface of PDA/NZVI@BC was increased, leading to the higher reaction rate of TC removal.

3.4 Reaction kinetics and mechanism of TC with PDA/NZVI@BC

3.4.1 Reaction kinetics

In this study, TC was removed rapidly in the first 10 min, and with the extension of reaction time, the removal efficiency was slowed down, indicating the occurrence of TC adsorption, the removal of TC with PDA/NZVI@BC was found not to follow the first-order or pseudo-first-order

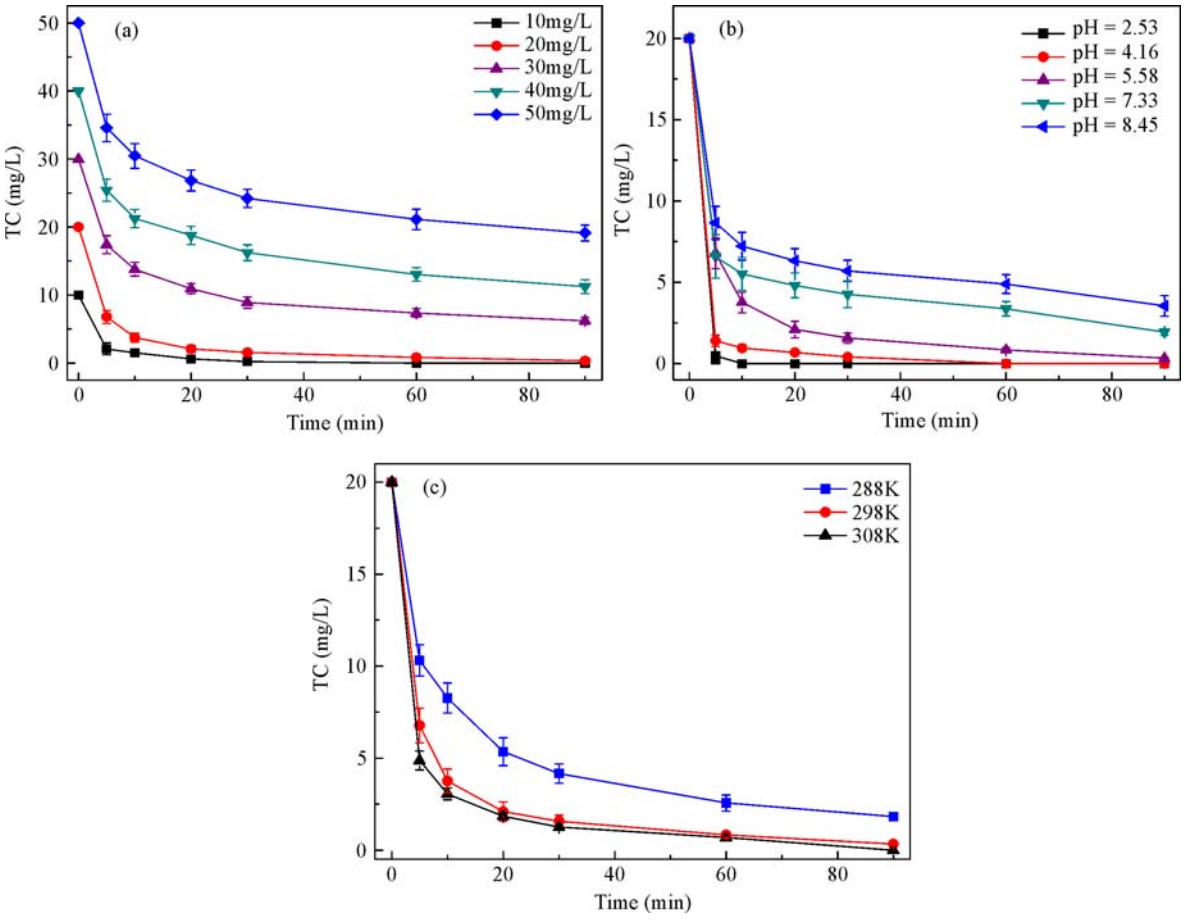

Fig. 6 Parameters affecting the degradation of TC: (a) initial TC concentration (PDA/NZVI@BC dosage = 1.0 g/L; pH = 5.58; t = 298 K); (b) pH value (C_0 = 20 mg/L; PDA/NZVI@BC dosage = 1.0 g/L; t = 298 K); (c) temperature (C_0 = 20 mg/L; PDA/NZVI@BC dosage = 1.0 g/L; pH = 5.58)

kinetics model. Therefore, a two-parameter pseudo-first-order decay model was employed to describe the reaction kinetics.

$$C_t = C_{ultimate} + (C_0 - C_{ultimate}) \times \exp(-kt) \quad (2)$$

where C_t (mg/L) is the concentration of TC in solution at reaction time t (min); $C_{ultimate}$ (mg/L) is the concentration of nonreactive TC in solution at infinite time; C_0 (mg/L) is the initial concentration of TC; k represents the reaction rate constant.

The calculated data in Table 1 show that all of the correlation coefficients R^2 were higher than 0.9763, indicating that the two-parameter pseudo-first-order decay model was fit for the experimental data well. The values of reaction rate constant k were in the range of 0.0065–0.1483 min^{-1}. The k value was increased with the decrease of pH value, proving that TC removal efficiency is higher under acidic conditions. The k value was found to increase with the decrease of initial TC concentration because that higher initial TC concentration inhibited the removal of TC. On the other hand, k value increased with the increase of reaction temperature, confirming slightly higher reaction temperature is more conducive for TC removal.

3.4.2 Degradation mechanism of TC with PDA/NZVI@BC

The UV–vis spectra were used to observe changes in degradation of TC by PDA/NZVI@BC at different reaction times. As can be seen in Fig. S2, the maximum absorption wavelength of TC appeared at around 380 nm and 275 nm, which was significantly reduced or disappeared with the increase of the reaction time. The by-products of TC degradation with PDA/NZVI@BC were qualitatively determined by LC-MS. The LC-MS spectra of TC, supernatant samples and the dissolved sample are shown in Fig.S3. The LC–MS analysis implied that m/z of the TC sample, supernatant samples and the dissolved sample were similar, mainly 461(m/z). Furthermore, in the supernatant and the dissolved sample, three anions with m/z of 405, 413 and 427 were observed. This proved that m/z of 405, 413 and 427 were the main intermediate product

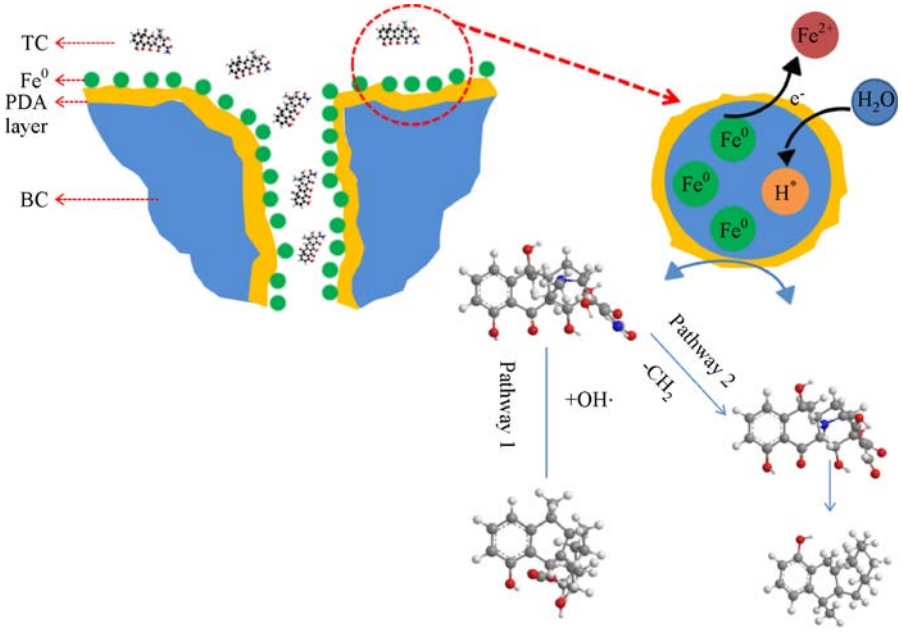

Fig. 7 Conceptual model for possible degradation pathways of TC by PDA/NZVI@BC

during reaction. The data of mass spectra of these samples reveal that PDA/NZVI@BC can absorb not only TC but also the degradation products. Base on LC-MS results, the main degradation products by PDA/NZVI@BC was proposed in Table.S2. Due to the low bond energy of N-C and the loss of hydroxyl group, TC produced the product 1 with m/z of 427. Because of the loss of amino group and hydroxyl group, the degradation product 1 resulted in the formation of product 2. Caused by the loss of carbonyl group and formyl group, product 3 was generated with the degradation of product 2.

Therefore, the possible removal pathways of TC by PDA/NZVI@BC were proposed in the light of identified products (Fig. 7).The hydrogenation reduction reaction in previous studies was considered as the primary removal mechanism of antibiotics by NZVI. The first step is the adsorption of TC onto reactive sites of PDA/NZVI@BC. Then the reduction of TC by PDA/NZVI@BC was induced by reactive species like H* that was resulted from the oxidation reduction process of NZVI. During degradation of TC, various chemical processes such as the loss of amino group, hydroxyl group, carbonyl group and formyl group were involved individually in pairs, or simultaneously.

4 Conclusions

For the first time, the composites of PDA/NZVI@BC were successfully synthesized. Compared with pristine NZVI, the reaction activity of as-synthesized PDA/NZVI@BC had been greatly improved. Based on the results, the major findings are summarized as follows: 1) the results obtained from SEM, XRD, XPS, and FTIR analyses indicated that loading NZVI onto BC/PDA facilitated the dispersion of NZVI; 2) PDA/NZVI@BC was with higher removal capacity for treatment of TC wastewater than that of pristine NZVI, and the removal capacities followed the order of PDA/NZVI@BC>BC/NZVI>NZVI>BC; 3) batch experiments indicated that the optimal NZVI to BC/PDA mass ratio is 1:2. TC removal efficiency decreased with increasing initial TC concentration and pH values, and it increased with the increase of solution temperature; 4) the synergistic effect between NZVI and BC/PDA is essential for improving TC removal efficiency; 5) degradation of TC by PDA/NZVI@BC followed the two-parameter pseudo-first-order decay kinetics model.

Acknowledgements This research was supported by the National Nature Science Foundation of China (Grant Nos. 51368025 and 51068011).

Electronic Supplementary Material Supplementary material is available in the online version of this article at https://doi.org/10.1007/s11783-018-1066-3 and is accessible for authorized users.

References

An B, Liang Q, Zhao D (2011). Removal of arsenic(V) from spent ion exchange brine using a new class of starch-bridged magnetite nanoparticles. Water Research, 45(5): 1961–1972

Arshadi M, Abdolmaleki M K, Mousavinia F, Foroughifard S, Karimzadeh A (2017). Nano modification of NZVI with an aquatic plant *Azolla filiculoides* to remove Pb(II) and Hg(II) from water: Aging time and mechanism study. Journal of Colloid and Interface Science, 486: 296–308

Arshadi M, Soleymanzadeh M, Salvacion J W, SalimiVahid F (2014).

Nanoscale Zero-Valent Iron (NZVI) supported on sineguelas waste for Pb(II) removal from aqueous solution: Kinetics, thermodynamic and mechanism. Journal of Colloid and Interface Science, 426: 241–251

Cai Z, Fu J, Du P, Zhao X, Hao X, Liu W, Zhao D (2018). Reduction of nitrobenzene in aqueous and soil phases using carboxymethyl cellulose stabilized zero-valent iron nanoparticles. Chemical Engineering Journal, 332: 227–236

Cao M, Wang L, Ai Z, Zhang L (2015). Efficient remediation of pentachlorophenol contaminated soil with tetrapolyphosphate washing and subsequent ZVI/Air treatment. Journal of Hazardous Materials, 292: 27–33

Chen S S, Hsu B C, Hung L W (2008). Chromate reduction by waste iron from electroplating wastewater using plug flow reactor. Journal of Hazardous Materials, 152(3): 1092–1097

Chen W R, Huang C H (2009). Transformation of tetracyclines mediated by Mn(II) and Cu(II) ions in the presence of oxygen. Environmental Science & Technology, 43(2): 401–407

Daghrir R, Drogui P (2013). Tetracycline antibiotics in the environment: A review. Environmental Chemistry Letters, 11(3): 209–227

Ding Y H, Floren M, Tan W (2016). Mussel-inspired polydopamine for bio-surface functionalization. Biosurface and Biotribology, 2(4): 121–136

Dong H, Deng J, Xie Y, Zhang C, Jiang Z, Cheng Y, Hou K, Zeng G (2017). Stabilization of nanoscale zero-valent iron (nZVI) with modified biochar for Cr(VI) removal from aqueous solution. Journal of Hazardous Materials, 332: 79–86

Dong H, Xie Y, Zeng G, Tang L, Liang J, He Q, Zhao F, Zeng Y, Wu Y (2016). The dual effects of carboxymethyl cellulose on the colloidal stability and toxicity of nanoscale zero-valent iron. Chemosphere, 144: 1682–1689

Feng J, Zhu B W, Lim T T (2008). Reduction of chlorinated methanes with nano-scale Fe particles: Effects of amphiphiles on the dechlorination reaction and two-parameter regression for kinetic prediction. Chemosphere, 73(11): 1817–1823

Ghauch A, Tuqan A, Assi H A (2009). Antibiotic removal from water: elimination of amoxicillin and ampicillin by microscale and nanoscale iron particles. Environmental Pollution, 157(5): 1626–1635

Guan X, Sun Y, Qin H, Li J, Lo I M, He D, Dong H (2015). The limitations of applying zero-valent iron technology in contaminants sequestration and the corresponding countermeasures: The development in zero-valent iron technology in the last two decades (1994–2014). Water Research, 75: 224–248

He F, Zhao D (2008). Hydrodechlorination of trichloroethene using stabilized Fe-Pd nanoparticles: Reaction mechanism and effects of stabilizers, catalysts and reaction conditions. Applied Catalysis B: Environmental, 84(3-4): 533–540

Hsieh W P, Pan J R, Huang C, Su Y C, Juang Y J (2010). Enhance the photocatalytic activity for the degradation of organic contaminants in water by incorporating TiO_2 with zero-valent iron. Science of the Total Environment, 408(3): 672–679

Jeong J, Song W, Cooper W J, Jung J, Greaves J (2010). Degradation of tetracycline antibiotics: Mechanisms and kinetic studies for advanced oxidation/reduction processes. Chemosphere, 78(5): 533–540

Jiang J, Zhu L, Zhu L, Zhang H, Zhu B, Xu Y (2013). Antifouling and antimicrobial polymer membranes based on bioinspired polydopamine and strong hydrogen-bonded poly(N-vinyl pyrrolidone). ACS Applied Materials & Interfaces, 5(24): 12895–12904

Lee H, Dellatore S M, Miller W M, Messersmith P B (2007). Mussel-inspired surface chemistry for multifunctional coatings. Science, 318 (5849): 426–430

Li J, Bao H, Xiong X, Sun Y, Guan X (2015a). Effective Sb(V) immobilization from water by zero-valent iron with weak magnetic field. Separation and Purification Technology, 151: 276–283

Li R, Jin X, Megharaj M, Naidu R, Chen Z (2015b). Heterogeneous Fenton oxidation of 2,4-dichlorophenol using iron-based nanoparticles and persulfate system. Chemical Engineering Journal, 264: 587–594

Li Y, Cheng W, Sheng G, Li J, Dong H, Chen Y, Zhu L (2015c). Synergetic effect of a pillared bentonite support on Se(VI) removal by nanoscale zero valent iron. Applied Catalysis B: Environmental, 174–175: 329–335

Loget G, Yoo J E, Mazare A, Wang L, Schmuki P (2015). Highly controlled coating of biomimetic polydopamine in TiO_2 nanotubes. Electrochemistry Communications, 52: 41–44

Lyu H, Zhao H, Tang J, Gong Y, Huang Y, Wu Q, Gao B (2018). Immobilization of hexavalent chromium in contaminated soils using biochar supported nanoscale iron sulfide composite. Chemosphere, 194: 360–369

Rodriguez-Mozaz S, Chamorro S, Marti E, Huerta B, Gros M, Sànchez-Melsió A, Borrego C M, Barceló D, Balcázar J L (2015). Occurrence of antibiotics and antibiotic resistance genes in hospital and urban wastewaters and their impact on the receiving river. Water Research, 69: 234–242

Sarmah A K, Meyer M T, Boxall A B (2006). A global perspective on the use, sales, exposure pathways, occurrence, fate and effects of veterinary antibiotics (VAs) in the environment. Chemosphere, 65(5): 725–759

Sever M J, Weisser J T, Monahan J, Srinivasan S, Wilker J J (2004). Metal-mediated cross-linking in the generation of a marine-mussel adhesive. Angewandte Chemie, 116: 43(4): 448–450

Shao B, Liu L F, Yang F L, Shan D N, Yuan H (2012). Membrane modification using polydopamine and/or PDA coated TiO_2 nano particles for wastewater treatment. Procedia Engineering, 44: 1431–1432

Shen W, Mu Y, Wang B, Ai Z H, Zhang L Z (2017). Enhanced aerobic degradation of 4-chlorophenol with iron-nickel nanoparticles. Applied Surface Science, 393: 316–324

Shi L N, Zhang X, Chen Z L (2011). Removal of chromium (VI) from wastewater using bentonite-supported nanoscale zero-valent iron. Water Research, 45(2): 886–892

Su H, Fang Z, Tsang P E, Fang J, Zhao D (2016b). Stabilisation of nanoscale zero-valent iron with biochar for enhanced transport and in-situ remediation of hexavalent chromium in soil. Environmental Pollution, 214: 94–100

Su H, Fang Z, Tsang P E, Zheng L, Cheng W, Fang J, Zhao D (2016a). Remediation of hexavalent chromium contaminated soil by biochar-supported zero-valent iron nanoparticles. Journal of Hazardous Materials, 318: 533–540

Su J, Lin S, Chen Z, Megharaj M, Naidu R (2011). Dechlorination of *p*-chlorophenol from aqueous solution using bentonite supported Fe/Pd

nanoparticles: Synthesis, characterization and kinetics. Desalination, 280(1-3): 167–173

Wang X, Chen C, Liu H, Ma J (2008). Preparation and characterization of PAA/PVDF membrane-immobilized Pd/Fe nanoparticles for dechlorination of trichloroacetic acid. Water Research, 42(18): 4656–4664

Xi Z Y, Xu Y Y, Zhu L P, Wang Y, Zhu B K (2009). A facile method of surface modification for hydrophobic polymer membranes based on the adhesive behavior of poly(DOPA) and poly(dopamine). Journal of Membrane Science, 327(1-2): 244–253

Yang K, Yue Q, Han W, Kong J, Gao B, Zhao P, Duan L (2015). Effect of novel sludge and coal cinder ceramic media in combined anaerobic–aerobic bio-filter for tetracycline wastewater treatment at low temperature. Chemical Engineering Journal, 277: 130–139

Yang L, Phua S L, Teo J K H, Toh C L, Lau S K, Ma J, Lu X (2011). A biomimetic approach to enhancing interfacial interactions: polydopamine-coated clay as reinforcement for epoxy resin. ACS Applied Materials & Interfaces, 3(8): 3026–3032

Yin W, Wu J, Li P, Lin G, Wang X, Zhu B, Yang B (2012a). Reductive transformation of pentachloronitrobenzene by zero-valent iron and mixed anaerobic culture. Chemical Engineering Journal, 210: 309–315

Yin W, Wu J, Li P, Wang X, Zhu N, Wu P, Yang B (2012b). Experimental study of zero-valent iron induced nitrobenzene reduction in groundwater: The effects of pH, iron dosage, oxygen and common dissolved anions. Chemical Engineering Journal, 184: 198–204

Yu J, Kan Y, Rapp M, Danner E, Wei W, Das S, Miller D R, Chen Y, Waite J H, Israelachvili J N (2013). Adaptive hydrophobic and hydrophilic interactions of mussel foot proteins with organic thin films. Proceedings of the National Academy of Sciences of the United States of America, 110(39): 15680–15685

Zabihi Z, Araghi H (2016a). Effect of functional groups on thermal conductivity of graphene/paraffin nanocomposite. Physics Letters, 380(45): 3828–3831

Zabihi Z, Araghi H (2016b). Monte Carlo simulations of effective electrical conductivity of graphene/poly(methyl methacrylate) nanocomposite: Landauer-Buttiker approach. Synthetic Metals, 217: 87–93

Zhu H, Jia Y, Wu X, Wang H (2009). Removal of arsenic from water by supported nano zero-valent iron on activated carbon. Journal of Hazardous Materials, 172(2-3): 1591–1596